

# Land cover time profiles from linear mixture models applied to MODIS images

P. Oliveira <sup>a</sup>, P. Gonçalves <sup>b</sup>, M. Caetano <sup>c</sup>,

<sup>a</sup> Institute of Statistic and Information Management (ISEGI), New University of Lisbon, Campus de Campolide, Lisbon, Portugal; pedroliveira@netcabo.pt

<sup>b</sup>INRIA Rhône-Alpes, 655 Av. de l'Europe, 38334 St. Ismier, France – paulo.goncalves@inria.fr

<sup>c</sup> Portuguese Geographic Institute, Av. Artilharia UM, 1099-052 Lisbon, Portugal – mario.caetano@igeo.pt

**Abstract** — A multi-temporal extension of Linear Mixture Models (LMM) is investigated. Applied to a full year sequence of MODIS 500 meters resolution images, time-varying Linear Mixture Models provide us with the inter-annual evolution of “vegetation”, “soil” and “shadow” sub-pixel components. Reported work is a descriptive analysis of the results and stands as a preliminary study towards automatic multi-temporal LMM based characterization and classification of land cover.

**Keywords:** MODIS, spectral mixture analysis, time series, temporal remote sensing, land cover

## 1 INTRODUCTION

The recent launch of the *Moderate Resolution Imaging Spectroradiometers* MODIS sensor opens a wide range of new possibilities on land cover characterization at regional scale.

MODIS sensors are mounted on two satellites from National Aeronautics and Space Administration (NASA): TERRA and AQUA launched on December 18, 1999 and on May 4, 2002, respectively. MODIS images correspond to high radiometric sensitivity (radiance) measured in 36 spectral bands that span a wavelength range from 0.4  $\mu\text{m}$  to 14.4  $\mu\text{m}$ . The two first bands (620-670 nm and 841-876 nm, primarily used for land/cloud/aerosols boundaries) are imaged at a nominal spatial resolution of 250 m at nadir. The next five bands (459-479 nm, 545-565 nm, 1230-1250 nm, 1628-1652 nm and 2105-2155 nm primarily used for land/cloud/aerosols properties) correspond to a 500 m pixel resolution. The remaining 29 bands are acquired at a coarser spatial resolution of 1 km. Furthermore, all images underwent a first level processing for geographic calibration and atmospheric surface reflectance correction.

Several studies have proved the advantages of multi-temporal images analysis for vegetation characterization, environmental monitoring and land cover mapping. As there is not one workbench methodology for exploring satellite images time series, several different approaches have been proposed in the literature (e.g. DeFries et al., 1997, Roberts et al., 1999, Boles et al. 2004, to cite but a few).

Spectral mixture analysis (SMA) has been used as a technique to bypass the coarse spatial resolution of satellites such as the Advanced Very High Resolution Radiometer (AVHRR) (e.g., Cross et al., 1991). SMA is based on the assumption that spectral signature of satellite images essentially results from a mixture of a small number of pure components with characteristic spectra (Adams et al., 1986, 1990). If so, it is then possible to use a limited number of components so that

mixtures of these component spectra adequately simulate the actual observations. The components used to model the spectra of each pixel have been designated in the literature as the endmembers.

A spectral mixture can be described as either a linear or a non-linear mixture of the components. The difference between linear and non-linear models is based on the types of interaction of the photons with the material within the pixel. In linear models (LMM) the electromagnetic energy interacts with a single component before being reflected by the surface.

The main objective of our current study is to assert ability of LMM applied to MODIS 500 m imagery time series, at classifying land covers. Taking advantage of the specific inter-annual dynamics of most important classes, we endeavour at maximising discrepancy between land cover types that share similar spectral reflectance responses for some periods of the year.

## 2 STUDY AREA AND DATA

The study area is the entire Portuguese continental territory. Our study relies on the MOD09A1 product, a 8 days composite surface reflectance images, freely available from MODIS Data Product web site (<http://modis.gsfc.nasa.gov>). We considered a full year observation period from February 2000 to January 2001. Surface reflectance measured within seven disjoint spectral bands (VIS+SWIR+MIR) were used and imaged at a nominal spatial resolution of 500 meters. Moreover, to enhance readability, original images acquired during the same month were re-composited to achieve a series of only twelve cloud-free images per spectral band for the full observation period. The compositing task relies on a local maximum NDVI criterion – *Maximum Value Composite* (e.g., Agrawal, 2003) – and integrates atmospheric information provided by the state quality assurance flag in MOD09A1 product.

CORINE Land Cover 2000 cartography (Instituto do Ambiente, 2005), derived from visual interpretation of LANDSAT ETM+ data, was used as auxiliary data to select both the training and the validating sets. We assigned to each land cover class, a set of at most 30 samples, each one representing a vector in  $[0,1]^7$  associated to one pixel of the reflectance composite images, i.e. a 500m-by-500m square area. Then, to ensure intra-class homogeneity, a dispersion criterion (based on minimum integrated squared distance between individuals and the mean population) was applied to perform a data clustering so as to remove possible outliers. The retained samples are finally randomly split into two

subsets of the same size: one for the training task, and the other for validation purpose.

Eleven Land Cover classes were defined according to the CLC2000 nomenclature. These classes received the following designations: (I) water bodies, (II) urban and industry, (III) barren land, (IV) natural grassland, (V) shrub land or herbaceous vegetation, (VI) needle leaf forest, (VII) broad leaf forest, (VIII) irrigated arable lands, (IX) non-irrigated arable lands, (X) burned forest area, (XI) new plantations or forest cuts.

### 3 MODEL

The basic assumption underlying Linear Mixture Models (LMM) is that most of the spectral variability in a satellite image stems from the mixture of elementary components with characteristic spectra. LMM, also referred to as spectral mixture analysis technique, aims thus at decomposing each image pixel into spectrally pure and distinct components: the so-called endmembers (Adams et al, 1986; Smith et al, 1990). Loosely, if not ill conditioned, the mixing rule allows for “zooming” at sub-pixel resolution, identifying within each coarse scale pixel, proportions of finer scale objects. Formally, the linear combination of a finite set of endmembers reads as follows:

$$DN_c = \sum_1^N F_n DN_{n,c} + E_c \quad (1)$$

where, within each spectral band  $c$ :

- $DN_c$  – stands for the image radiance,
- $N$  – is the number of endmembers,
- $F_n$  – is the relative fraction of endmember  $n$ ,
- $DN_{n,c}$  – is the endmember  $n$  inner radiance,
- $E_c$  – represents the residual fitting error term.

Furthermore, in our model we chose to force the decomposition to be complete, imposing that the relative endmembers proportions  $F_n$  not only satisfy to a conservation-like property (fractions sum to one), but also lie within the interval  $[0,1]$ . Notice though, that this later condition is not a proviso for LMM.

The LMM was built with three endmembers: green vegetation, bare soil and shadow (Fig. 1). Each of these pure elements is characterized by an expectable theoretical spectrum, upon which we based our endmember selection strategy: that is to find pixels that globally optimize over space and time, a particular reflectance criterion. More precisely:

- vegetation endmember was identified among all pixels with maximum NDVI value as the one with minimum medium infra-red reflectance (band 7);
- bare soil endmembers was identified among all pixels with minimum NDVI absolute value as the one with maximum medium infra-red reflectance (band 7);
- shadow endmembers was identified among all pixels with minimum NDVI absolute value as the one with minimum medium infra-red reflectance (band 7);

The endmembers used to unmix all MODIS composited images were the same, in order to allow the intra-annual comparison of EM fractions.

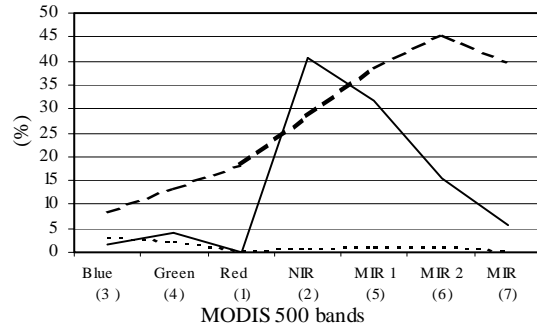


Figure 1. Endmember characteristic reflectance spectra. Full line corresponds to vegetation, dashed line to soil and dotted line to shadow.

To a posteriori assess goodness-of-fit and accuracy of our endmembers selection, we applied the LMM of equation (1) to all image pixels and for the 12 dates. The root mean square error computed at the pixel level showed that the fitting error  $E_c$  in expression (1) has a median reasonably negligible as compared to the total reflectance  $DN_c$ , corroborating thus the good adequacy between Linear Mixture Models and our reflectance data.

### 4 MIXTURE TIME SERIES: DESCRIPTIVE ANALYSIS

#### 4.1 Land cover characterization

We applied the Linear Mixture Model on the training sets determined for all land cover classes. The resulting mixture time series are presented in Fig 2 and 3.

At first glance, the vegetation fraction response allows to define two distinct sets of land cover classes. One — comprising: irrigated lands, non irrigated lands, broadleaf forests and natural grasslands — shows a high inter-annual variation (relative proportions vary with amplitudes ranging from 25 up to more than 50% during a full year period). This is not surprising, for all these classes share a common phenology that is highly seasonal dependent. More precisely though, the absolute phase of these pseudo-periodic oscillations allows for clearly isolate among this first set of classes, the irrigated land class that, in contrast with the remainders, is subject to artificial irrigation at summer time. As a result, a phase shift  $\Delta\varphi \approx \pi$  appears between this human dependent land cover and all other natural vegetation classes.

The complementary set — gathering water, urban, barren, shrub land and needle leaf forests — is characterized by small amplitude variations of the vegetation fraction (maximum deviation is less than 25%). Yet, closer views at the vegetation mean fraction values of this class reveals the existence of two new subsets: On one hand, a vegetation dominant group (barren, shrub land and needle leaf forests) corresponding to an overall vegetation fraction larger than 25% over the full year period. On the other hand, a weak vegetation land cover type (annual mean fraction less or equal to 25%) easily secludes water and urban classes.

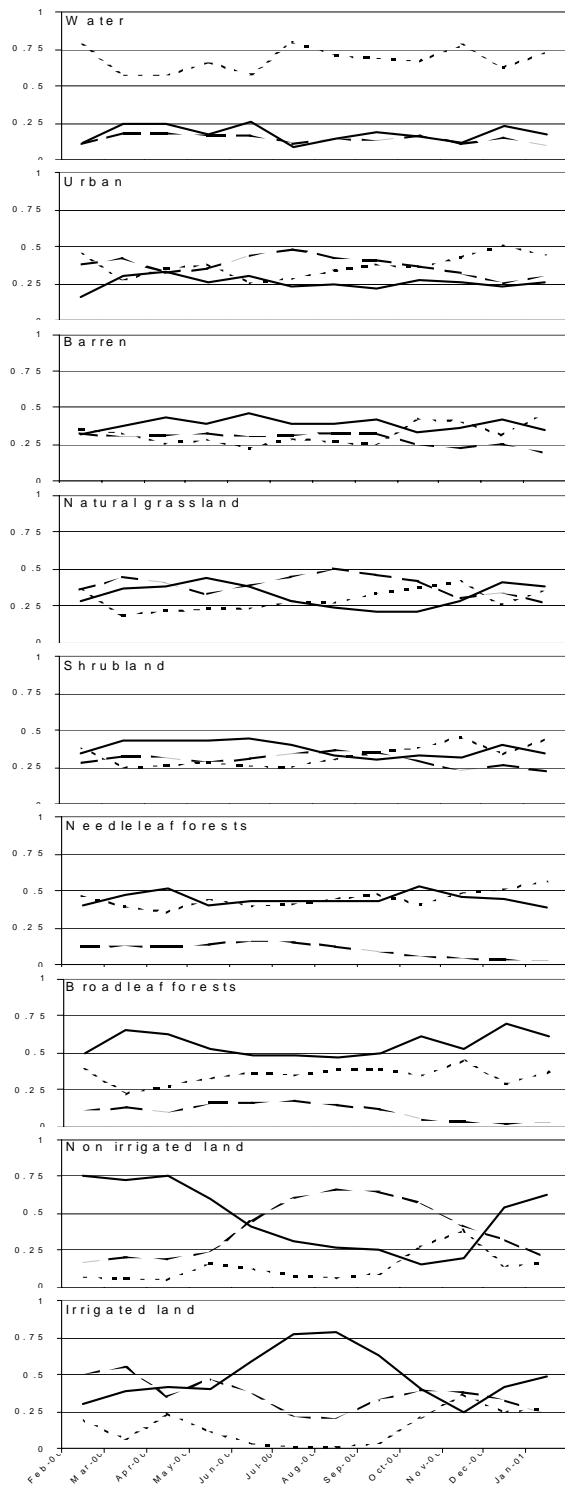


Figure 2. Time profiles of the fractions corresponding to a three endmembers Linear Mixture Model. Each plot corresponds to one of the 9 considered land cover classes. Full lines, dashed lines and dotted lines correspond to vegetation, soil and shadow fractions, respectively.

Now, considering the soil fraction, a similar dichotomy seems to apply. For classes expressing significant seasonal vegetation dynamic, it is most likely that soil should be a complementary component as far as land occupation is concerned. Thus, it is not surprising that for those classes (namely, irrigated lands, non irrigated lands, broadleaf forests and natural grasslands) soil fraction trend will roughly reproduce the main variations of the vegetation fraction, but with opposite slopes.

Strikingly, the urban class, although it does not belong to the set of pseudo-periodic vegetation changes, shows a significant soil fraction drop between summer time (50%) and winter time (25%), whereas the vegetation ratio remains reasonably constant (25%) during this same period.

We then need to examine the shadow fraction evolution to explain such an apparent contradiction between vegetation and soil components. As a preliminary remark, recall that shadow (or water) endmembers aim at modeling not only the effective presence of water, but also at quantifying the amount of dark zones. Consequently, this component is particularly sensitive to illumination conditions, that is, to cloud shadow and to the mean sun angle. Said this, it is noticeable that in all classes, the shadow mixture component substantially increases at fall time. So, now, looking back to the urban zone, since vegetation fraction actually remains constant, the shadow raise occurring at autumn must be balanced by the unique free left parameter, hence the soil fraction decrease.

More profitably though, the shadow component can help to discriminate forest from shrubland (Caetano et al., 1997). In our case, albeit needle leaf and broad leaf forests do differ by their vegetation time profiles, their dissimilitude is far more notable when comparing the shadow fractions mean values.

Finally, we would like to report on two methodological hurdles. The first one, inherent to the multi-temporal approach, is the difficulty to find training pixels acquired under good atmospheric condition during the entire observation period. Sometimes, the compositing process is not sufficient at removing cloud occlusion, then, a denoising technique (e.g. median filter, wavelet thresholding) might be necessary to correct local aberrant reflectance measurements. In any case, special care should be paid to the state quality assurance flag supplied in MOD09A1 product.

Our second concern stems from the model itself where we forced the endmember fractions to sum to one and to be bounded ( $0 \leq F_n \leq 1$ ). These constraints deem natural in such a mixture model, and yet, they often create singular symmetries between two of the three mixture time profiles. Obvious from a mathematical viewpoint (the three random variables are not independent), this effect may be embarrassing to interpret from a cover land cover use prospect.

#### 4.2 Land cover change detection

Multi-temporal analyses are particularly adapted at identifying singular events responsible for non-stationarity in time series. Hence, quite naturally, we foresee that time evolution of

mixture ratio will be notably helpful at determining “accidental” events such as wild fires and forest clear cuts. However, this land cover changes detection faces an additional difficulty when it comes to determine the corresponding prototype profiles. Indeed, because of the non-synchrony of the events, it is not possible to average different sample time profiles in order to reduce noise and intra-variability of the data. Therefore, the classifier will have to cope with this extra degree of freedom, and most likely we will have to resort to the theory of detection of a signal with unknown parameter(s). Fig. 3 displays the typical profiles for two kinds of land cover changes caused by a forest fire and a forest clear cut. In both cases, a sharp discontinuity in the vegetation fraction signal precisely indicates the date at which the accidental event occurred.

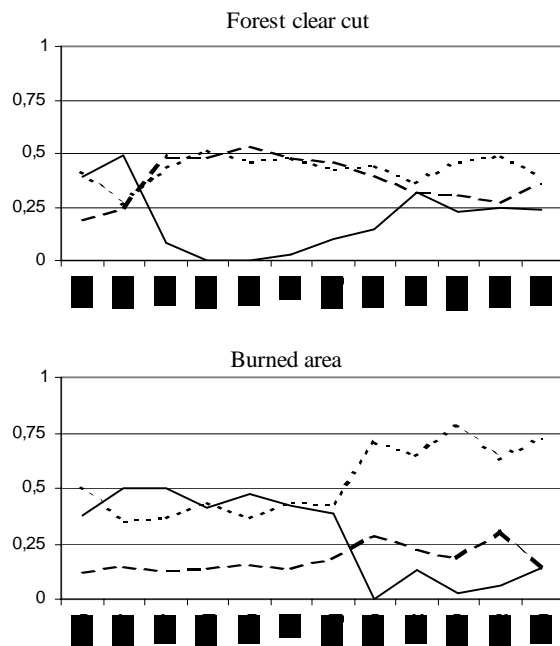


Figure 3. Time profiles of the endmembers fractions for a forest area affected by a clear cut (top) and by a fire (bottom). Full lines, dashed lines and dotted lines correspond to vegetation, soil and shadow fractions, respectively.

## 5 CONCLUSIONS AND FORTHCOMING WORK

The work reported here, is a preliminary step towards automatic land cover classification based on multi-temporal mixture profiles. As such, this article merely focuses on a qualitative description of the mixture components, and strived at showing how vegetation, soil and shadow responses, used as complement of standard indices (e.g., NDVI, EVI...) can sensibly refine remote sensing scores at a sub-pixel resolution.

## 6 REFERENCES

- J. B. Adams, and M. O. Smith, “Spectral mixture modelling: A new analysis of rock and soil types at the Viking Lander 1 Site”, *Journal of Geophysical Research*, Vol 91, p.p. 8098-8112, 1986.
- J. B. Adams, M. O. Smith, and A. R. Gillespie, “Imaging spectroscopy: data analysis and interpretation based on spectral mixture analysis.”. *Remote Geochemical Analysis: Elemental and Mineralogical Composition*, Pieters and Englert (Eds), p.p. 3-39, 1990.
- S. Agrawal, P. K. Joski, Y. Shukla, and P. S. Roy, “SPOT VEGETATION multi-temporal data for classifying vegetation in south central Asia,” *Current Science*, Vol 84, 1440-1448, 2003.
- M. Caetano, T. Oliveira, J. Paúl, M. Vasconcelos, and J. Pereira, “Mapping shrublands and forest with multispectral satellite images based on spectral unmixing of scene components,” *Earth Surface Remote Sensing*, G. Cecchi, E.T. Engman, and E. Zilioli (Eds). *Proceedings of SPIE 3222*, p.p. 4-14, 1997.
- A. M. Cross, J. J. Settle, N. A. Drake, AND R. T. M. Paivinen, “Sub pixel measurement of tropical forest cover using AVHRR data,” *International Journal of Remote Sensing*, Vol 12, p.p. 1119-1129, 1991.
- Instituto do Ambiente, “CLC2000 Portugal”, Technical Report, 2005.
- M. O. Smith, S. L. Ustin, J. B. Adams, and A. R. Gillespie, “Vegetation in deserts: I. A regional measure of abundance from multispectral images”, *Remote Sensing of Environment* Vol 31, p.p. 1-26, 1990.
- D. A. Roberts, G. T. Batista, J. L. G. Pereira, E. K. Waler, and B. W. Nelson, “Change identification using multitemporal spectral mixture analysis: applications in eastern Amazonia,” *Remote Sensing Change Detection - Environmental Monitoring Methods and Applications*, R. S. Lunetta, and C. D. Elvidge (Eds), Taylor & Francis Editions, p.p. 137-159, 1999.
- S. H. Boles, X. Xiao, J. Liu, Q. Zhang, S. Munkhtuya, S. Chen, and D. Ojima, “Land cover characterization of Temperate East Asia using multi-temporal VEGETATION sensor data,” *Remote Sensing of Environment*, Vol 90, p.p. 47-489, 2004.
- R. DeFries, M. Hansen, M. Steininger, R. Dubayah, R. Sohlberg, and J. Townshend, “Subpixel Forest Cover in Central Africa from Multisensor, Multitemporal Data,” *Remote Sensing of Environment*, Vol 60, p.p. 228-246, 1997.